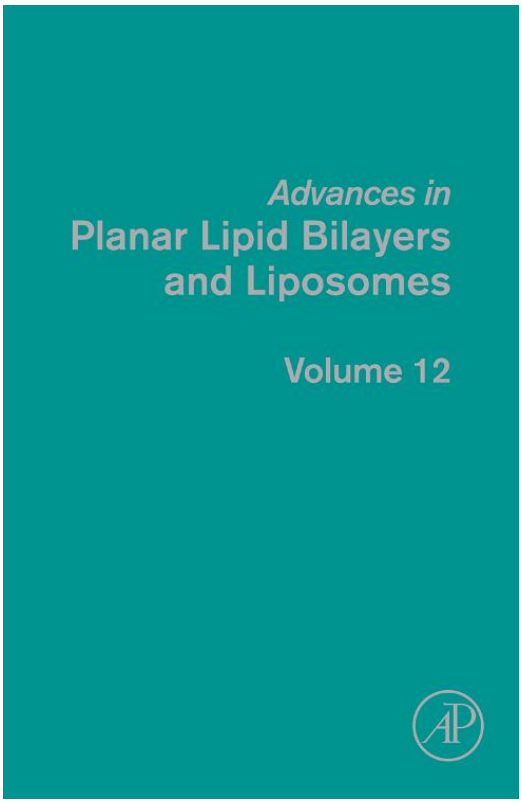

From: France Sevs̆ek, Membrane Elasticity from Shape Fluctuations of Phospholipid Vesicles, In Dr. Ales̆ iglic and Dr. H.T. Tien editor: "Advances in Planar Lipid Bilayers and Liposomes," Vol. 12.
Burlington: Academic Press, 2010, pp.1-20.
ISBN: 978-0-12-381266-7 © Copyright 2010,
Elsevier Inc. Academic Press.

CHAPTER ONE

Membrane Elasticity from Shape Fluctuations of Phospholipid Vesicles

France Sevšek*

Contents

Abstract

Thermal shape fluctuations of nearly spherical phospholipid vesicles are studied by Monte Carlo calculations. The constraints of constant volume and surface area are treated in two ways: (i) by strictly considering only the phase space of the allowed shapes and (ii) by adding the appropriate elastic term to the energy. In the limit of high elastic constants, the two approaches yield the same results, which also agree well with the predictions of the effective tension approximation. The importance of the cutoff value ℓ_{max} is shown. The "elastic approach" allows us to establish the transition from a free fluctuation regime to a constrained one.

* Corresponding author. Tel.: +386 13001112; Fax: +386 13001119
E-mail address: france.sevsek@zf.uni-lj.si

Faculty of Health Sciences, University of Ljubljana, Ljubljana, Slovenia

Advances in Planar Lipid Bilayers and Liposomes, Volume 12
ISSN 1554-4516, DOI: 10.1016/S1554-4516(10)12001-8

1. Introduction

Phospholipid vesicles have been intensively studied as a model for biological membranes and also for their own sake. They are usually categorized on the basis of their size, as small (<50 nm), large (50–1000 nm), and giant vesicles (>1 μm). According to their membrane thickness, they can be unilamellar if the membrane is composed of a single bilayer or multilamellar, when the membrane is made of a number of bilayers entrapping some of the solvent [1].

Giant unilamellar vesicles (GUV) with the radius in the micrometer range, which are the object of interest in this work, can be quite easily prepared and can be readily observed by optical microscopy and manipulated by micropipettes. This is a system at the border between the microscopic and the macroscopic worlds. As structures delimited by very thin fluid membranes, they exhibit some interesting properties, including shape fluctuations, that are driven by the thermal energy. They have been used as model systems for studying the dynamics and structural properties of many cellular processes, particularly those related to membrane elastic properties [2]. Phospholipid vesicles have also been applied as a means for the encapsulation [3] and transport of different molecules within a living organism.

Phospholipid vesicles form spontaneously in water when a thin film of amphiphilic phospholipid molecules closes upon itself minimizing the energy due to the membrane rigidity and the one arising from the edge tension [4]. There exist a variety of classical experimental methods to prepare phospholipid vesicle suspensions [1]. For experimental purposes, giant vesicles of up to 50 μm radius are usually prepared by hydrating a thin phospholipid film that is formed by spreading a chloroform/methanol solution of phospholipid to a substrate and subsequently allowing the solvent to evaporate under reduced pressure. Applying very low frequency voltage to the solution of the nascent vesicles has been shown to greatly enhance the hydrating process and increase the number of monolayer vesicles [5,6].

The phospholipid membranes are virtually an incompressible and impermeable two dimensional liquid. The shape of a phospholipid vesicle is thus mainly controlled by the bending elasticity of the membrane [7].

The bending modulus (k_c) of the phospholipid membrane as introduced by Helfrich [7] can be determined experimentally by observing the shape fluctuations of vesicles. The standard technique is to observe the vesicles by an inverted optical microscope using phase contrast technique. Using an attached CCD camera, digitizing hardware, and suitable software, a large number of images of a fluctuating vesicle are recorded. Their shapes can be then determined by an outline, following algorithm [8]. Such a procedure is essentially limited by the finite integration time of the camera and the space resolution of the CCD sensor. These effects must be considered in the final analysis [9].

By the Fourier analysis of the vesicle cross-sections, the mean square amplitudes of the normal-mode displacements $\left(\left\langle u_m^2 \right\rangle\right)$ are determined as a function of wave numbers [8,10–12]. Fitting the calculated values of $\left\langle u_m^2 \right\rangle$ to these data yields the value of k_c.

Traditionally, the effective tension approach, as introduced by Milner and Safran [13], is used to analyze the shape fluctuations of nearly spherical vesicles. It is based on the spherical harmonics expansion of the vesicle shape deviations from a sphere where only the second-order terms are retained. In this approximation, the mean square amplitudes of the fluctuational modes are inversely proportional to the fourth power of the wave number (ℓ^{-4}). The equilibrium tension is interpreted as an effective tension that is treated as a fitting parameter. In this way, the bending moduli (k_c) of a wide range of phospholipids have been determined. As there is quite a variation between the reported results, it seems that the measured values depend not only on the type of phospholipid used, but also on the experimental procedure where the data collection and the theoretical approximation used in the analysis are of the utmost importance. It is thus of special interest to investigate the validity of the latter.

From mechanical experiments [14], it is known that the value of the membrane expansivity modulus is so large that thermal excitations cannot measurably alter the membrane surface area. Furthermore, as a result of osmotically active molecules that are always present, the transmembrane pressure difference is very sensitive to small volume changes. It is thus reasonable to expect that the volume of a vesicle and the surface area of its membrane remain constant during the observation time. For this reason, thermal fluctuations of phospholipid vesicles at constant volume and the membrane area are of principal interest. In general, this problem does not seem to have a simple analytical solution. The most straightforward approach is by Monte Carlo method. Bivas *et al.* [15] preformed the calculations for a small range of volume to area ratios and limiting the procedure exclusively to $\ell_{\max} = 20$ spherical harmonic terms in the expansion of nearly spherical vesicle shapes. As the later theoretical work by Seifert [16] indicated the importance of the number of the spherical harmonic terms $\ell_{\max}$, more detailed investigation of these fluctuations began to be carried out. Later, the analysis of Pécreaux *et al.* [9] showed that the high wave number modes did not depend on the actual vesicle shape and could be reliably determined experimentally. In studying biological membranes, more complicated systems began to attract interest: membranes with embedded proteins [17] and those with nanotubular protrusions [18]. In general, non-equilibrium vesicles and the ones with active proteins in the membrane [19] are expected to exhibit different fluctuation spectra.

In the present work, we combine the second-order approximation for the vesicle shape with the constant volume and area constraints using the Monte Carlo method for a large range of cutoff values ($\ell_{\max}$) as well as

volume to area ratios. We start by defining the basic relations for a vesicle of a nearly spherical shape and introduce the effective tension in a simple way. Here, we mainly follow the well-established path. The introductory part of this work is concluded with a short discussion on the Monte Carlo method. Two approaches to Monte Carlo calculations of thermal fluctuations are then presented. The "delta function approach" treats the constant volume and area requirement strictly by limiting the phase space to only those shapes that do not violate the constraints. Using the "elastic approach", we understand the treatment of the constraints by considering additional elastic terms in the energy of a vesicle. The two approaches are expected to yield the same results in the limit of large elastic constants. This is shown to be indeed the case. In the final section, we also compare our Monte Carlo results with the effective tension approximation. It is to be noted that such a procedure can be easily extended to more complicated cases of fluctuating vesicles.

2. Nearly Spherical Vesicles

2.1. Vesicle Shape

The shape of a nearly spherical vesicle is conveniently expressed in terms of spherical harmonics

$$R(\theta,\phi) = R_s\left(1 + \sum_{\ell=0}^{\ell_{\max}} \sum_{m=-\ell}^{m=\ell} u_{\ell m} Y_{\ell m}(\theta,\phi)\right), \tag{1}$$

where $R(\theta, \varphi)$ is the distance from origin of the coordinate system to the membrane and the constant R_s is introduced in such a way that all coefficients are small. In what follows, the origin of the coordinate system is chosen to be at the geometrical center of the membrane, and R_s is defined as the radius of the equivalent sphere, that is, the radius of the sphere with the same unstretched surface area as the studied vesicle. $Y_{\ell m}(\theta, \varphi)$ are normalized spherical harmonics:

$$Y_{\ell m}(\theta,\varphi) = N_{\ell m} P_{\ell m}(\cos\theta) e^{\mathrm{i}m\varphi}, \tag{2}$$

with $P_{\ell m}(\cos\theta)$ being the associated Legendre functions and

$$N_{\ell m} = \sqrt{\frac{2\ell+1}{4\pi}\frac{(\ell-|m|)!}{(\ell+|m|)!}} \tag{3}$$

the appropriate normalization factors.

The coefficients $u_{\ell m}$ are complex numbers:

$$u_{\ell m} = \alpha_{\ell m} + \mathrm{i}\beta_{\ell m}. \tag{4}$$

As the distance $R(\theta, \varphi)$ in Eq. (1) is real, the coefficients are interrelated

$$\alpha_{\ell,-m} = (-1)^m \alpha_{\ell m}, \quad \beta_{\ell,-m} = -(-1)^m \beta_{\ell m}. \tag{5}$$

Thus for each ℓ, there are $2\ell + 1$ independent coefficients. In this chapter, we prefer to use the real coefficients that are defined as

$$x_{\ell m} = \alpha_{\ell m}\sqrt{2}, \quad x_{\ell,-m} = \beta_{\ell m}\sqrt{2} \tag{6}$$

for $m > 0$ and $x_{\ell 0} = \alpha_{\ell 0}$. With this notation we get

$$u_{\ell m} u^*_{\ell m} = \frac{1}{2}\left(x^2_{\ell m} + x^2_{\ell -m}\right) \quad \text{for } m > 0 \tag{7}$$

$$u^2_{\ell 0} = x^2_{\ell 0}. \tag{8}$$

Because in the second-order approximation, there is no dependence on index m (see below), it is convenient to define

$$u^2_\ell = \sum_{m=-\ell}^{m=\ell} u_{\ell m} u^*_{\ell m} = \sum_{m=-\ell}^{m=\ell} (-1)^m u_{\ell m} u_{\ell,-m} = \sum_{m=-\ell}^{m=\ell} x^2_{\ell m}. \tag{9}$$

Experimentally, only the cross-section of a fluctuating vesicle can be observed under the microscope. For vesicles of nearly spherical shapes this cross-section can be approximated by the equatorial one which is simply obtained from Eq. (1) by taking $\theta = (\pi\ /2)$.

$$\begin{aligned} R\left(\theta = \frac{\pi}{2}, \varphi\right) &= R_\mathrm{s}\left(1 + \sum_{\ell=0}^{\ell_\mathrm{max}} \sum_{m=-\ell}^{m=\ell} u_{\ell m} N_{\ell m} P_{\ell m}(0) e^{im\varphi}\right) \\ &= R_\mathrm{s}\left(1 + \sum_{m=-\ell_\mathrm{max}}^{m=\ell_\mathrm{max}} \mathrm{e}^{im\varphi} \sum_{\ell=|m|}^{\ell_\mathrm{max}} u_{\ell m} N_{\ell m} P_{\ell m}(0)\right) \\ &= R_\mathrm{s}\left(1 + \sum_{m=-\ell_\mathrm{max}}^{m=\ell_\mathrm{max}} \mathrm{e}^{im\varphi} u_m\right). \end{aligned} \tag{10}$$

The Fourier coefficients of the observed cross-section are thus

$$u_m = \sum_{\ell=|m|}^{\ell_\mathrm{max}} u_{\ell m} N_{\ell m} P_{\ell m}(0). \tag{11}$$

The appropriate values of the associated Legendre functions can be calculated as [20]

$$P_{\ell m}(\cos\pi/2) = P_{\ell m}(0) = 2^{|m|}\frac{1}{\sqrt{\pi}}\cos\left[\frac{\pi}{2}(\ell+m)\right]\frac{\Gamma\left(\frac{\ell}{2}+\frac{|m|}{2}+\frac{1}{2}\right)}{\Gamma\left(\frac{\ell}{2}-\frac{|m|}{2}+1\right)} \quad (12)$$

2.2. Elastic Energy of a Vesicle

The elastic energy of a phospholipid vesicle can be generally expressed as [21]

$$W = W_B + \frac{1}{2}\frac{K}{A_0}(A-A_0)^2 + \frac{1}{2}\frac{K_V}{V_0}(V-V_0)^2 + \frac{1}{2}\frac{K_r}{A_0}(\Delta A - \Delta A_0)^2, \quad (13)$$

where W_B is the energy due to the pure bending of the phospholipid membrane, and the next three terms represent the energy due to the isotropic lateral extension of the bilayer, the vesicle volume change, and the relative expansion of the two membrane monolayers, respectively. K, K_V, and K_r are the appropriate elastic constants, and A_0, V_0, and ΔA_0 the surface area, volume, and the area difference between the two monolayers, in the relaxed state.

The bending energy of a thin symmetric phospholipid bilayer is expressed as [7]

$$W_B = \frac{k_c}{2}\oint (C_1 + C_2)^2 dA, \quad (14)$$

where k_c stands for the membrane bending modulus, C_1 and C_2 are the principal curvatures of the bilayer, and the integration is done over the neutral surface of the lipid bilayer.

For vesicles of nearly spherical shapes, we can calculate the bending energy by inserting the spherical harmonics expansion (Eq. (1)) into Eq. (14) and neglecting all terms of higher than quadratic order in coefficients $u_{\ell m}$. With this second-order approximation, the bending energy becomes [13,22]

$$W_B = 8\pi k_c\left[1 + \frac{1}{16\pi}\sum_{\ell=0}^{\ell_{max}}\lambda_\ell(\lambda_\ell - 2)u_\ell^2\right], \quad (15)$$

where $\lambda_\ell \equiv \ell(\ell+1)$.

In the same way, the surface area (A), volume (V), and the area difference (ΔA) between the two layers of a vesicle can be calculated. If they are normalized relative to a sphere with radius R_s, we get

$$a = \frac{A}{4\pi R_s^2} = 1 + \frac{2u_0}{\sqrt{4\pi}} + \frac{1}{8\pi}\sum_{\ell=0}^{\ell_{max}} (\lambda_\ell + 2)u_\ell^2, \tag{16}$$

$$v = \frac{V}{\frac{4}{3}\pi R_s^3} = 1 + \frac{3u_0}{\sqrt{4\pi}} + \frac{6}{8\pi}\sum_{\ell=0}^{\ell_{max}} u_\ell^2, \tag{17}$$

$$\Delta a = \frac{\Delta A}{8\pi R_s h} = 1 + \frac{u_0}{\sqrt{4\pi}} + \frac{1}{8\pi}\sum_{\ell=0}^{\ell_{max}} \lambda_\ell u_\ell^2. \tag{18}$$

Here, h is the distance between the neutral planes of the two phospholipid layers.

From Eqs. (16)–(18), we see that in this approximation a, v, and Δa are not independent. Their relation is

$$\Delta a = a - (v - 1)/3. \tag{19}$$

Thus, for the shape of nearly spherical vesicles, we need to consider only the normalized surface area and the volume of the vesicle as independent parameters.

3. Effective Tension

The equilibrium shape of a nearly spherical elastic vesicle can be easily determined by the minimization of Eq. (13). For nearly spherical vesicles, we can neglect all terms of a higher than second order in $u_{\ell m}$, together with ${u_0}^2$. We define the membrane surface tension (Σ), pressure (P), and the tension due to relative area difference (Σ_Δ) in the usual way

$$\Sigma = \frac{K}{A_0}(A - A_0), \quad P = \frac{K_V}{V_0}(V - V_0), \quad \Sigma_\Delta = \frac{K_r}{A_0}(\Delta A - \Delta A_0). \tag{20}$$

At the equilibrium, we get from $\partial W/\partial u_0 = 0$ the following relation:

$$2R_s\Sigma + R_s^2 P + 2h\Sigma_\Delta = 0. \tag{21}$$

With this expression, we can introduce the generalized equilibrium tension as

$$\gamma \equiv -R_s^2(\Sigma + R_s P) = R_s^2\left(\Sigma + \frac{h}{R_s}\Sigma_\Delta\right), \tag{22}$$

so that at equilibrium we obtain for $\ell \neq 0$:

$$\left(\frac{\partial W}{\partial u_{\ell m}}\right)_{\mathrm{eq}} = u_{\ell m}(\lambda_\ell - 2)(k_\mathrm{c}\lambda_\ell + \gamma) = 0. \tag{23}$$

It is worth noting that the generalized equilibrium tension of Eq. (22) reduces to the well known expression [16] if the energy term due to the relative stretching of the two monolayers is omitted (i.e., $K_\mathrm{r} = 0$): $\gamma = {R_\mathrm{s}}^2\Sigma$.

From Eq. (23), we see that for $\ell \geq 2$, only one coefficient u_ℓ can be nonzero at equilibrium: the one for which $k_\mathrm{c}\lambda_\ell = -\gamma$. As for the other coefficients, the second derivative of the elastic energy is

$$\left(\frac{\partial^2 W}{\partial u_{\ell m}^2}\right)_{\mathrm{eq}} = (\lambda_\ell - 2)(k_\mathrm{c}\lambda_\ell + \gamma), \tag{24}$$

And the stable equilibrium state is obtained with only nonzero coefficients: u_0 and u_{2m}. The generalized equilibrium tension is thus $\gamma = -6k_\mathrm{c}$.

From this, the mean square amplitudes of the spherical harmonic modes $\left(\left\langle u_{\ell m}^2\right\rangle\right)$ due to thermal fluctuations about the equilibrium shape can be easily estimated. If the fluctuational amplitudes are small, the elastic potential can be considered as harmonic, determined by Eq. (24). If there is no interaction between different spherical harmonics modes, the values of $\left\langle u_{\ell m}^2\right\rangle$ are calculated using the equipartition theorem as

$$\left\langle u_{\ell m}^2\right\rangle = \frac{kT}{(\lambda_\ell - 2)(k_\mathrm{c}\lambda_\ell + \gamma)}, \tag{25}$$

Combining Eq. (25) with Eq. (11), the mean square amplitudes of the Fourier coefficients of the equatorial cross-section are determined as

$$\left\langle u_m^2\right\rangle = kT \sum_{\ell=|m|}^{\ell_{\max}} \frac{N_{\ell m}^2 P_{\ell m}^2(0)}{(\lambda_\ell - 2)(k_\mathrm{c}\lambda_\ell + \gamma)}. \tag{26}$$

We can extend this treatment to the fluctuations at constant (average) volume and surface area. This is done by replacing the generalized equilibrium tension γ by an effective tension parameter σ/k_c in such a way that Eq. (25) will give the correct volume and surface area if inserted into Eqs. (17) and (16) [15]. The effective tension parameter (σ) thus depends also on the number of spherical harmonics expansion terms ($\ell_{\max}$). It is always larger than the equilibrium tension $\gamma/k_\mathrm{c} = -6$ and tends to infinity as the volume approaches that of a sphere ($v = 1$). The meaning of the cutoff value $\ell_{\max}$ and its relation to the membrane tension is similar to Debye temperature in solid state physics. If we insist on harmonic potential for all the wave lengths, as small as they are, some artificial cutoff value must

be introduced to compensate for this approximation. That is, as the wave lengths become smaller, the thin membrane and continuum approximations break down, and the simple harmonic treatment cannot be extended so far. Anyhow, the cutoff value $\ell_{\max}$ is still a meaningful parameter that, together with the normalized volume, characterizes the vesicle.

The results of this "effective tension approximation" are included in Figs. 1–3, where they are represented by solid lines.

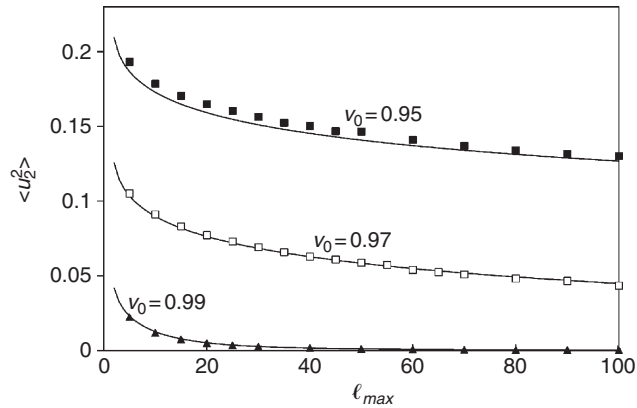

Figure 1 Dependence of $\langle u_2^2 \rangle$ on $\ell_{\max}$ for normalized volumes 0.95 (squares), 0.97 (empty squares), and 0.99 (triangles) as calculated by the Monte Carlo method for $k_c = 10^{-19}$ J and $T = 300$ K. The solid lines were obtained by the effective tension approximation.

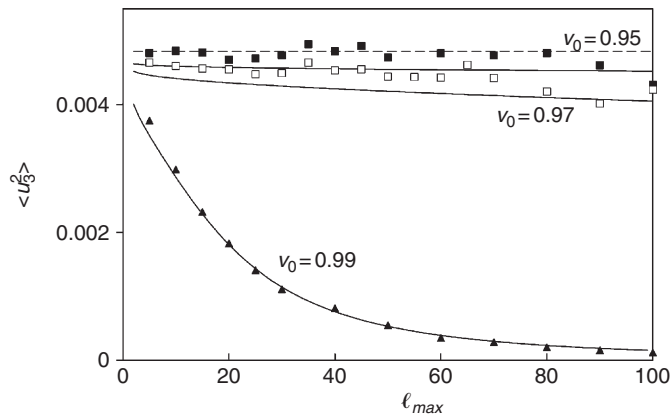

Figure 2 Dependence of $\langle u_3^2 \rangle$ on $\ell_{\max}$ for normalized volumes 0.95 (squares), 0.97 (empty squares), and 0.99 (triangles) as calculated by the Monte Carlo method for $k_c = 10^{-19}$ J and $T = 300$ K. The solid lines were obtained by the effective tension approximation whereas the dashed line represents the effective tension approximation for $\sigma = -6$.

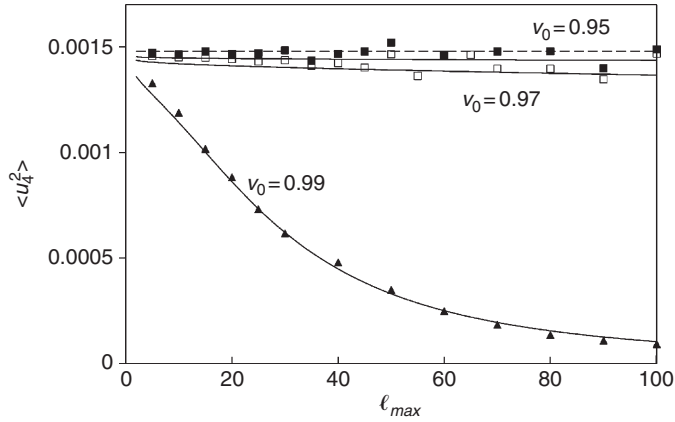

Figure 3 Dependence of $\langle u_4^2 \rangle$ on $\ell_{\max}$ for normalized volumes 0.95 (squares), 0.97 (empty squares),and 0.99 (triangles) as calculated by the Monte Carlo method for $k_c = 10^{-19}$ J and $T = 300$ K. The solid lines were obtained by the effective tension approximation whereas the dashed line represents the effective tension approximation for $\sigma = -6$.

Equation (26) is usually used to analyze the experimental data, where k_c and σ are treated as fitting parameters. For vesicles that exhibit detectably large fluctuations, σ is normally obtained in the range of -6 to about 100.

This treatment is expected to be valid for vesicles that are sufficiently nonspherical so that the fluctuations are confined mostly to the vicinity of the equilibrium state but are still close enough to being spherical to justify the second-order approximation.

The other limiting case, when the vesicle shape approaches the spherical one, can also be determined. When it is close to being spherical, the fluctuations are governed predominantly by the two constraints, and the bending energy can be neglected. Using the same procedure as outlined above, one gets by setting $k_c = 0$:

$$\langle u_{\ell m}^2 \rangle = \frac{kT}{(\lambda_\ell - 2)\gamma}. \tag{27}$$

Eliminating u_0 from the two constraints (Eqs. (17) and (16)) and considering that the excess area is equally distributed [13] among all $N = (\ell_{\max} + 1)^2 - 4$ available modes, we get from Eq. (27)

$$\gamma = \frac{3NkT}{16\pi(1 - v_0)}. \tag{28}$$

Thus, for vesicles close to a spherical shape, the effective tension is expected to be proportional to $\ell_{\max}{}^2$ [16].

4. Metropolis Monte Carlo Calculation

The Monte Carlo method studies thermodynamic systems by stochastic computer simulation [23,24]. It is devised such that the trajectory in the phase space probes mainly those states that are statistically most important.

If the state of a phospholipid vesicle is determined by a set of coefficients $x_{\ell m}$ (configuration x) and has the energy $E(x)$, then the thermodynamic average of $A(x)$ is

$$\langle A \rangle = \frac{\int_\Omega A(x) e^{-E(x)/kT} dx}{\int_\Omega e^{-E(x)/kT} dx}, \tag{29}$$

where the $(\ell_{\max} + 1)^2$ dimensional integration is over the allowed phase space volume Ω.

For any large non-trivial system, the total number of possible configurations is very large, and straightforward sampling of configurations in Eq. (29) is not possible. Here, the Monte Carlo method proves to be useful.

In this work, we consider two approaches to treat the constant volume and area constraints. Using the first one, which we call "delta function approach", we limit the available phase space by calculating two variables chosen *a priori* from the constraints, whereas when using the second, "elastic" approach, we consider the vesicle to be elastic, with large energy penalties imposed on the vesicle surface area and volume changes. We shall see that the results of both methods agree well.

4.1. Delta Function Approach

In Eq. (29), the integration must be done over the whole phase space, which is allowed by the constant volume and surface area constraints. The most straightforward approach is to replace in the integrals two variables (e.g., x_{L1M1} and x_{L2M2}) by the integration over volume and area.

$$\int_\Omega A(x) \mathrm{e}^{-E(x)/kT} dx = \int \delta(v - v_0)\delta(a - a_0) A(x) e^{-E(x)/kT} dx \tag{30}$$

$$\int_\Omega A(x) \mathrm{e}^{-E(x)/kT} dx = \int \delta(v - v_0)\delta(a - a_0) A(x) e^{-E(x)/kT} dx' J dv da \tag{31}$$

where dx' stands for the integration over remaining $x_{\ell m}$ variables and J is the absolute value of the Jacobian determinant.

$$J = \left| \frac{\partial x_{L_1 M_1}}{\partial a} \frac{\partial x_{L_2 M_2}}{\partial \upsilon} - \frac{\partial x_{L_1 M_1}}{\partial \upsilon} \frac{\partial x_{L_2 M_2}}{\partial a} \right|. \tag{32}$$

Besides the constant volume and area, the three coefficients x_{1m} are also constant. They are set to zero to ensure that $\bar{x} = \bar{y} = \bar{z} = 0$, which is identical to choosing the origin of the coordinate system in the membrane geometrical center. The shape of a vesicle is thus defined by a, υ, and $(\ell_{\max} + 1)^2 - 5$ coefficients $x_{\ell m}$. At the beginning of every Monte Carlo calculation, we arbitrarily choose two pairs L_1, M_1 and L_2, M_2. The coefficients corresponding to them are treated as dependent variables and are in each Monte Carlo step calculated from a and υ and all the remaining coefficients.

At every step, a coefficient $x_{\ell m}$ is randomly picked from $(\ell_{\max} + 1)^2 - 5$ possible ones. Its value is changed from $x_{\ell m}$ to $x_{\ell m} + \delta$, where δ is chosen randomly in the predetermined interval $(-z_{\ell m}, z_{\ell m})$. The appropriate values of x_{L1M1} and x_{L2M2} are then calculated. If both these values are real, the standard Metropolis procedure is applied, using Eq. (15) to calculate the change of bending energy ΔW_B. If ΔW_B is negative, the new configuration is accepted. But when ΔW_B is positive, the change is accepted with the probability $e^{-(\Delta W_B / \kappa T)}$. For this purpose, a random number is chosen between 0 and 1, and the new configuration is accepted only when this number is less than $e^{-(\Delta W_B / \kappa T)}$. Otherwise, the new configuration is rejected and the previous one is counted once more. The values of the intervals $z_{\ell m}$ are chosen in such a way that the acceptance rate is about (1/2).

After a large number of steps, the trajectory thus generated samples the configurations in accordance with the canonical Boltzmann distribution of configurations [24]. We can thus calculate the needed average values by a simple arithmetic averaging of the appropriate values (e.g., $x_\ell^2(i)$) multiplied by the absolute value of the Jacobian (J_i) at every visited point of the phase space.

$$\langle x_\ell^2 \rangle = \sum_{i=1}^{i=N} x_\ell^2(i) J_i \Big/ \sum_{i=1}^{i=N} J_i. \tag{33}$$

The first N_0 steps were rejected in order to reduce the dependence on the initial values. Then the averages were calculated for N steps, with N_0 typically being 10^5 to 10^6, and N from 10^7 to 10^8 steps. Of N calculated configurations, typically 100 equally spaced ones were stored. From them, the standard deviations of the parameters were calculated, and the plot of stored values was used to monitor whether the fluctuations were well thermalized.

At every Monte Carlo step, we also calculated the values of u_m^2 using Eq. (11). This yielded the average values of the square Fourier coefficients of

the vesicle cross-section. These correspond to the experimentally obtainable data and can, alternatively, also be calculated from the $\langle u_{\ell m}^2 \rangle$ values.

Most of the calculations were preformed on a PC type computer using Linux operating system. In these calculations, the portable pseudorandom number generator Ran3, based on a subtractive method, was used [25,26]. It has a very long period and no evident defects. To eliminate the possible implementation defects, a thorough statistical test of the program was performed [27].

4.2. Elastic Approach

Except for the three x_{1m} variables fixing the origin of the coordinate system, all the remaining $(\ell_{\max} + 1)^2 - 3$ ones are considered to be independent. The two constraints are taken into account by adding to the vesicle energy an "elastic" term as in Eq. (13).

$$W = W_{\mathrm{B}} + \kappa_a (a - a_0)^2 + \kappa_v (v - v_0)^2. \tag{34}$$

The fluctuational spectra are calculated by the standard Metropolis procedure as described in the previous section. This approach enables us to study systematically the influence of the elastic constants on the thermal fluctuation spectra. Anyhow, without much loss of generality, we report in this work only the cases when the two elastic constants κ_a and κ_v were taken to be equal.

5. Results and Discussion

Calculations have been performed for a vesicle with the membrane bending modulus $k_c = 10^{-19}$ J, a typical value for phospholipid bilayers [6]. As stated above, the normalized surface area was chosen to be $a_0 = 1$. The vesicle shape fluctuations were thus determined only by the normalized volume (v_0), which was varied from 0.95 to 0.999.

At first, we studied the influence of the cutoff number of expansion coefficients ($\ell_{\max}$) on the calculated mean square values of the spherical harmonics modes. By varying $\ell_{\max}$ from 5 to 100, we noticed that all the calculated values of $\langle u_\ell^2 \rangle$ showed a clear dependence on $\ell_{\max}$. It was more pronounced for more spherical shapes, that is, for those with larger v_0, as seen in Figs. 1–3. Here, the points represent the results of the Monte Carlo calculation by the "delta function approach" while the lines were obtained by the effective tension approximation as described above. The striking agreement indicates that these two approximations are very similar. The discrepancy is noticed mostly for quite flaccid vesicles. When a vesicle

is sufficiently deformed to have large excess of area, as for instance at $v = 0.95$, its fluctuations are expected to be confined principally to the vicinity of its equilibrium shape which is defined by the coefficients u_0 and u_2. The mean square value of the coefficient u_2 is composed of static and fluctuational part. It is thus not surprising that $\langle u_2^2 \rangle$ as calculated by the Monte Carlo method is slightly larger than the one given by the effective tension approximation. This is evident from the top curve in Fig. 1. In the case of quite flaccid vesicles, the Monte Carlo values of $\langle u_\ell^2 \rangle$ for $\ell > 2$ are, for small ℓ,closer to those obtained by $\sigma = -6$ (dashed lines in Figs. 2 and 3) than to those given by the effective tension approximation. It is also interesting to note that the Monte Carlo $\langle u_\ell^2 \rangle$ values calculated for $\ell_{\max} = 20$ agree well with those given in [15], although their procedure was slightly different from ours.

The results of the "elastic" Monte Carlo calculations are shown in Figs. 4 and 5 for two different volumes. Note that, for the sake of clarity, the scale of the horizontal axis is logarithmic. Here, the dependence of the amplitudes of spherical modes on the elastic constants κ_a and κ_u was studied.

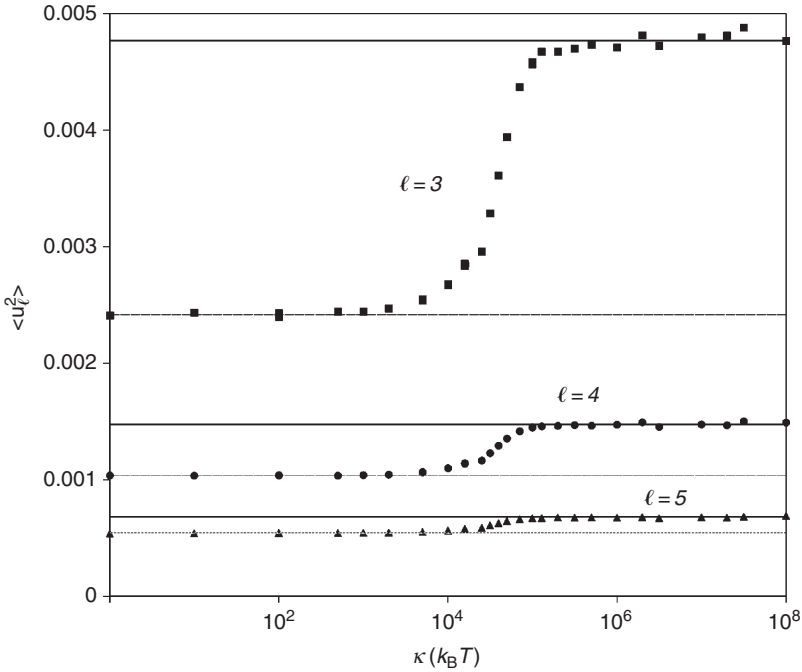

Figure 4 The results of the Monte Carlo calculation for $v_0 = 0.95$. Points were obtained by the "elastic approach" for $\ell_{\max} = 20$ as a function of the elastic constants ($k \equiv k_a = k_v$). The dashed lines are the result of the "delta function approach," whereas the dotted ones represent the free fluctuation regime.

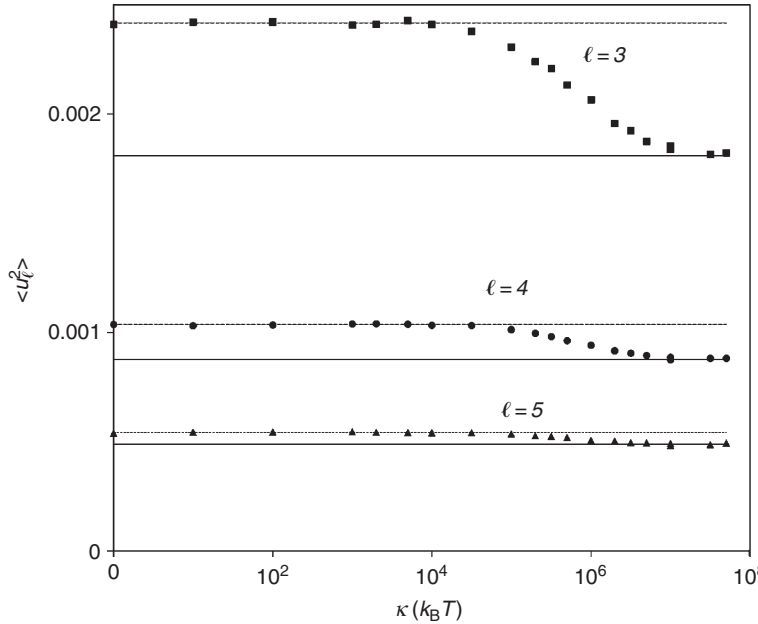

Figure 5 The results of the Monte Carlo calculation for $v_0 = 0.99$. Points were obtained by the "elastic approach" for $\ell_{max} = 20$ as a function of the elastic constants ($\kappa \equiv \kappa_a = \kappa_v$). The dashed lines are the result of the "delta function approach," whereas the dotted ones represent the free fluctuation regime.

For the reason of simplicity, the two constants were always chosen to be equal ($\kappa \equiv \kappa_a$ and κ_u). As expected, for a given normalized volume (v) and cutoff (ℓ_{max}), there are three different regions. For small values of the elastic constants, the fluctuations are determined mainly by the membrane bending modulus (k_c). The mean squares of the spherical harmonics amplitudes of a freely fluctuating vesicle can be determined from Eq. (25) if the tension (σ) is set to zero. These values are represented by dotted lines in Figs. 4 and 5. On the other side, the large values of the elastic constants result in the constrained fluctuations. It was observed that here the mean squares of the spherical harmonic modes yielded the same values as the "delta function approach." The latter are shown as solid lines. Between these two regions, there is an interval of intermediate fluctuations. As seen from the calculated data, the width of this intermediate region depends on the normalized volume of the vesicle.

Comparing Figs. 4 and 5, we note that the introduction of the volume and area constraints can either increase or decrease the shape fluctuations of a vesicle. If its shape is close to that of a sphere, the constraints result in smaller fluctuational amplitudes as given by the bending energy of an

unconstraint vesicle. For the flaccid vesicle, the constraints may result in the equilibrium deformation that could already be larger than the unconstrained fluctuations. Generally, when at a given cutoff value $\ell_{\max}$, the normalized volume is such that the effective tension (σ) is negative, the constrained fluctuations are larger than the free ones. On the contrary, when the vesicle shape is sufficiently close to that of a sphere, the effective tension σ becomes positive, and the constant area and volume constraints reduce the amplitudes of the fluctuations. For a given $\ell_{\max}$, there exists a volume for which the fluctuational amplitudes in the two limiting regions are the same. For instance, for $\ell_{\max} = 20$, the effective tension is zero if $v_0 = 0.9883$. This result was also confirmed by our Monte Carlo calculations. This is evident from Figs. 6 and 7 as well, where the coefficients $\langle u_2^2 \rangle$ and $\langle u_3^2 \rangle$ are plotted as a function of the elastic constant κ for some values of the normalized vesicle volume.

Finally, we tried to answer the question: supposing that the fluctuations of observed vesicles can be well described by the second-order approximation of constrained fluctuations, how reliable are the experimentally determined values of the bending modulus? For this purpose, we treated the mean square values of the Fourier coefficients $\langle u_m^2 \rangle$ that were obtained by

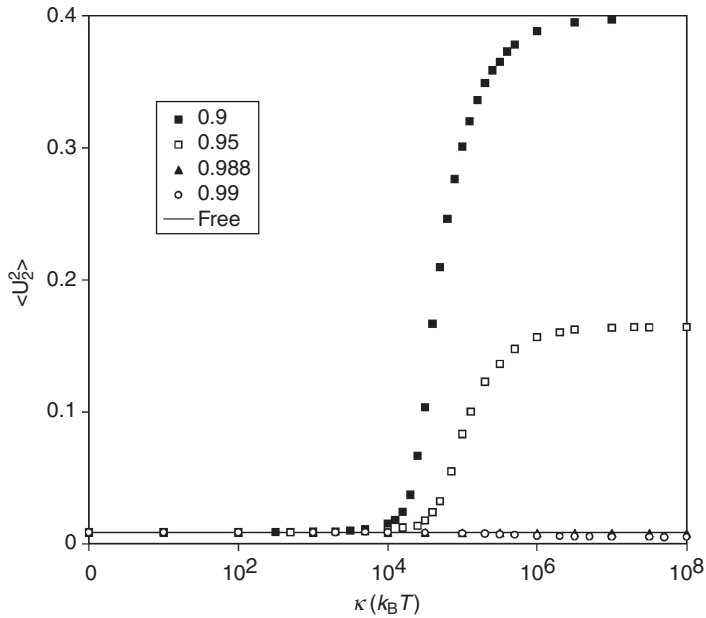

Figure 6 Dependence of $\langle u_2^2 \rangle$ on elastic constants κ as calculated by the Monte Carlo method for $k_c = 10^{-19}$ J, $T = 300$ K, $\ell_{\max} = 20$, and various values of the normalized volume. The horizontal line represents the analytical result for a freely fluctuating vesicle.

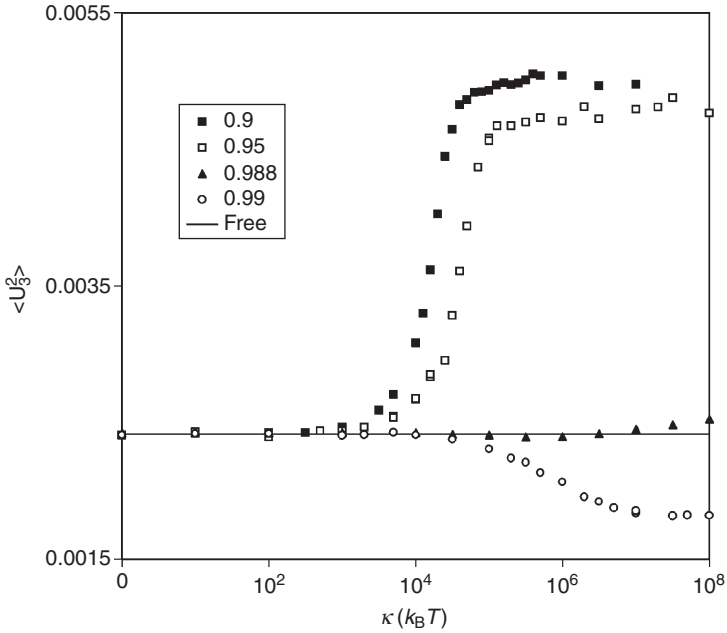

Figure 7 Dependence of $\langle u_3^2 \rangle$ on elastic constants κ as calculated by the Monte Carlo method for $k_c = 10^{-19}$ J, $T = 300$ K, $\ell_{max} = 20$, and various values of the normalized volume. The horizontal line represents the analytical result for a freely fluctuating vesicle.

our Monte Carlo calculations as if they were experimental data. We fitted Eq. (26) to $\langle u_m^2 \rangle$ for $2 < m \leq 10$ to get the value of the bending modulus and effective tension. The number of the terms used in the transformation of spherical harmonic coefficients $\langle u_\ell^2 \rangle$ to the Fourier coefficients of the contour (ℓ_{max} in Eq. (26)) does not influence the result, as long as it is sufficiently large. It was always taken to be 100, the value normally used in our experimental analysis. This procedure gave us the values of the bending moduli that differed from the "true" one by less than 3% for all the Monte Carlo results obtained with $\ell_{max} > 20$.

6. Conclusions

An effective tension model of the thermal fluctuations of phospholipid vesicles has been derived and its results compared with the results of the Monte Carlo calculations, considering strict volume and surface area conservation. The two approaches yielded very similar results, especially for

vesicles close to a spherical shape. Here the cutoff value of $\ell_{\max}$ was related to the effective tension and the normalized volume of the vesicle. The fluctuations of the vesicles of shapes close to that of a sphere are mostly dominated by the normalized volume whereas those of more flaccid vesicles are mainly governed by the membrane bending modulus. It was shown that the intermediate region was well reproduced by the Monte Carlo calculations, which showed continuous transition between the two analytically determined limits. It is thus expected that it will also be possible to extend this method to the study of the thermal fluctuations of more complex systems.

REFERENCES

[1] D. Lasic, The mechanism of vesicle formation, Biochem. J. 256(1) (1988) 1–11.
[2] S. Svetina, B. Žekš, Shape behavior of lipid vesicles as the basis of some cellular processes, Anat. Rec. 268 (2002) 215–225.
[3] L.M. Dominak, C.D. Keating, Polymer encapsulation within giant lipid vesicles, Langmuir 23 (2007) 7148–7154.
[4] E. Hernández-Zapata, L. Luciano Martínez-Balbuena, I. Santamaría-Holek, Thermodynamics and dynamics of the formation of spherical lipid vesicles, J. Biol. Phys. 35 (2009) 297–308.
[5] M. Angelova, S. Soléau, P. Méléard, J. Faucon, P. Bothorel, Preparation of giant vesicles by external ac electric fields. Kinetics and applications, Prog. Colloid Polym. Sci. 89 (1992) 127–131.
[6] V. Heinrich, R. Waugh, A piconewton force transducer and its application to measure the bending stiffness of phospholipid membranes, Ann. Biomed. Eng. 24 (1996) 595–605.
[7] W. Helfrich, Elastic properties of lipid bilayers: theory and possible experiments, Z. Naturforsch. 28C (1973) 693–703.
[8] F. Sevšek, Shape determination of attached fluctuating phospholipid vesicles, Comput. Methods Programs Biomed. 73 (2004) 189–194.
[9] D. Pécreaux, H.G. Dobereiner, J. Prost, J.F. Joanny, P. Bassereau, Refined contour analysis of giant unilamellar vesicles, Eur. Phys. J. 13 (2004) 277–290.
[10] H. Engelhardt, H. Duwe, E. Sackmann, Bilayer bending elasticity measured by Fourier analysis of thermally excited surface undulations of flaccid vesicles, J. Phys. Lett. 46 (1985) L395–L400.
[11] H. Duwe, J. Kaes, E. Sackmann, Bending elastic moduli of lipid bilayers: modulation by solutes, J. Phys. France 51 (1990) 945–962.
[12] I. Bivas, P. Hanusse, P. Bothorel, J. Lalanne, O. Aguerre-Chariol, An application of the optical microscopy to the determination of the curvature elastic modulus of biological and model membranes, J. Phys. 48 (1987) 855–867.
[13] S. Milner, S. Safran, Dynamical fluctuations of droplet microemulsions and vesicles, Phys. Rev. A 36 (1987) 4371–4379.
[14] E. Evans, D. Needham, Physical properties of surfactant bilayer membranes: thermal transitions, elasticity, rigidity, cohesion and colloidal interactions, J. Phys. Chem. 91 (1987) 4219–4228.
[15] I. Bivas, L. Bivolarski, M. Mitov, A. Derzhanski, Correlations between the form fluctuation modes of flaccid quasispherical lipid vesicles and their role in calculation

of the curvature elastic modulus of vesicle membrane. Numerical results, J. Phys. II France 2 (1992) 1423–1438.
[16] U. Seifert, The concept of effective tension for fluctuating vesicles, Z. Phys. B 97 (1995) 299–309.
[17] M. Fosnaric, A. Iglic, T. Slivnik, V. Kralj-Iglic, Flexible membrane inclusions and membrane inclusions induced by rigid globular proteins, Adv. Planar Lipid Bilayers Liposomes 7 (2008) 143–168.
[18] Š. Perutkova, V. Kralj-Iglič, M. Frank, A. Iglič, Mechanical stability of membrane nanotubular protrusions influenced by attachment of flexible rod-like proteins, J. Biomech. 43 (2010) 1612–1617.
[19] S. Ramaswamy, J. Toner, J. Prost, Nonequilibrium fluctuations, traveling waves, and instabilities in active membranes, Phy. Rev. Lett. 84 (2000) 3494–3497.
[20] M. Abramowitz, I.A. Stegun, Handbook of Mathematical Functions, Dover Publications, New York, 1965.
[21] F. Sevšek, S. Svetina, B. Žekš, The effect of membrane elasticity on the shape of nearly spherical phospholipid vesicles, in: R. Lipowsky, D. Richter, K. Kremer (Eds.), The Structure and Conformation of Amphiphilic Membranes, Springer-Verlag, Berlin, Heidelberg, 1992, pp. 101–104.
[22] W. Helfrich, Size distributions of vesicles: the role of the effective rigidity of membranes, J. Phys. France 47 (1986) 321–329.
[23] K. Binder (Ed.), Monte Carlo Methods in Statistical Physics, Springer Verlag, Berlin, 1979.
[24] D. Chandler, Introduction to Modern Statistical Mechanics, Oxford University Press, USA, 1987.
[25] W. Press, S.A. Teukolsky, Portable random number generators, Comput. Phys. 6 (1992) 522–524.
[26] W. Press, S. Teukolsky, W. Vetterling, B. Flannery, Numerical Recipes in C Cambridge University Press, New York, 1992.
[27] D. Knuth, The Art of Computer Programming, Addison-Wesley, Massachusetts, 1969.

This page intentionally left blank